

# Multi-modality imaging of structure and function combining spectral-domain optical coherence and multiphoton microscopy

Claudio Vinegoni<sup>a</sup>, Tyler Ralston<sup>a,b</sup>, Wei Tan<sup>a</sup>, Wei Luo<sup>a</sup>, Daniel L. Marks<sup>a,b</sup>, Stephen A. Boppart<sup>a,b,c</sup>

<sup>a</sup>Beckman Institute for Advanced Science and Technology

<sup>b</sup>Department of Electrical and Computer Engineering

<sup>c</sup>Departments of Bioengineering, Medicine  
University of Illinois at Urbana-Champaign

## ABSTRACT

We have constructed an integrated optical microscope that allows for the simultaneous image acquisition from multiple optical imaging modalities. The microscope consists primarily of hardware for spectral-domain optical coherence microscopy (OCM), multi-photon microscopy (MPM), and second harmonic generation microscopy. The unique configuration of the integrated microscope allows for the acquisition of both anatomical and functional imaging information with particular emphasis in the fields of tissue engineering and tumor biology. By overlaying the structural image obtained from OCM on the functional image obtained simultaneously from MPM (i.e., fluorescent markers imply functional proteins), a more comprehensive view of different tissues can be obtained. In addition, the contemporary analysis of the spectroscopic features enhances contrast in OCM by differentiating different cell and tissue components.

Keywords: Optical Coherence Microscopy, Multiphoton Microscopy, Spectral-Domain Detection, Spectroscopy

## 1. INTRODUCTION

Optical coherence tomography (OCT) is very useful as a non-invasive and high resolution imaging technique for locating and diagnosing pathological tissue. However, primarily only the linear characteristics of the tissue, such as scattering, birefringence, absorption, and refractive index contribute in producing contrast. Moreover, these properties can be very similar in different tissues. The unfortunate result is that these linear scattering properties for pathological tissue, when probed by OCT, are often morphologically and optically similar to the scattering properties present in normal tissue. For example, although morphological differences between normal and neoplastic tissues may be obvious at later stages of tumor development, it is very difficult, if not impossible, to optically detect early-stage tumors.

In recent years, different approaches have been used in order to solve this problem. In particular, new OCT techniques that exploit molecular differences, for example the use of exogenous contrast agents targeted to bind to specific molecules, or techniques that exploit coherent nonlinear optical methods in order to identify endogenous molecular properties (i.e., second harmonic generation, CARS imaging) have been developed<sup>1</sup>. Another alternative approach, as presented in this paper, consists of combining two or more different optical imaging techniques that provide different yet complementary information, such as by combining OCM with MPM.

Multi-photon microscopy (MPM) has become a well-established optical imaging technique since its first exploitation more than a decade ago<sup>2</sup>. The technique allows thin optical sectioning deep from within thick scattering samples. Optical coherence microscopy (OCM)<sup>3</sup> extends the capabilities of OCT and confocal microscopy by combining high-sensitivity coherence-gated detection with confocal optical sectioning. The result is an improvement in the rejection of unwanted scattered light generated from points outside of the imaging plane. A dramatic enhancement of the image contrast is therefore possible.

It is highly desirable to combine both OCM and MPM imaging functions into a single instrument. MPM is based on the detection of fluorescence emitted by endogenous or exogenous markers whereas OCM delivers information on the scattering properties of the sample, commonly without the addition of exogenous agents. These two modalities therefore

provide different imaging contrast mechanisms, increasing the information extracted. In fact, the unique configuration of the proposed setup and the opportunity to obtain both anatomical and functional imaging information simultaneously will potentially make the integrated microscope an attractive imaging tool that could be widely exploited in multiple fields. One specific application is in the field of tissue engineering, where the combined modalities can serve as an enabling diagnostic tool for future studies in the growth and organization of engineering tissues, and in cell-cell and cell-matrix interactions. Other applications exist in the fields of tumor biology or plant biology, where the localization and interaction of different proteins tagged with fluorescent proteins is of interest relative to the development and growth of the local microenvironment.

## 2. EXPERIMENTAL SETUP

The setup used in this work is shown in Fig. 1. The light source consist of a frequency-doubled Nd:YVO<sub>4</sub>-pumped Ti:sapphire laser with a center wavelength of 800 nm, a bandwidth of 60 nm, and an average power on the sample of 5 mW at an 80 MHz repetition rate. To compensate for the pulse lengthening due to the high dispersion of our objective (Olympus, water-immersion, 20x, 0.9 NA), pulses are first pre-compensated using a double-fold prism path. The beam is then guided to a scan head that consist of two galvo-controlled mirrors for high speed acquisition, and then matched to the back-aperture of our objective where the beam is finally focused in the sample. The galvanometer driven mirrors allows for high speed scanning in the x-axis (1 kHz) and slower speed scanning along the y-axis (10 Hz). The sample is fixed on a holder attached to a 3D translation stage that allows for large scanning areas, such as for imaging large tissue sections or *in vivo* animal imaging. In addition, the z-axis translation allows for multiple image acquisition and subsequently for 3D volume rendering. The titanium:sapphire laser source functions both as an excitation source for two-photon fluorescence and as a low-coherence source for OCM.

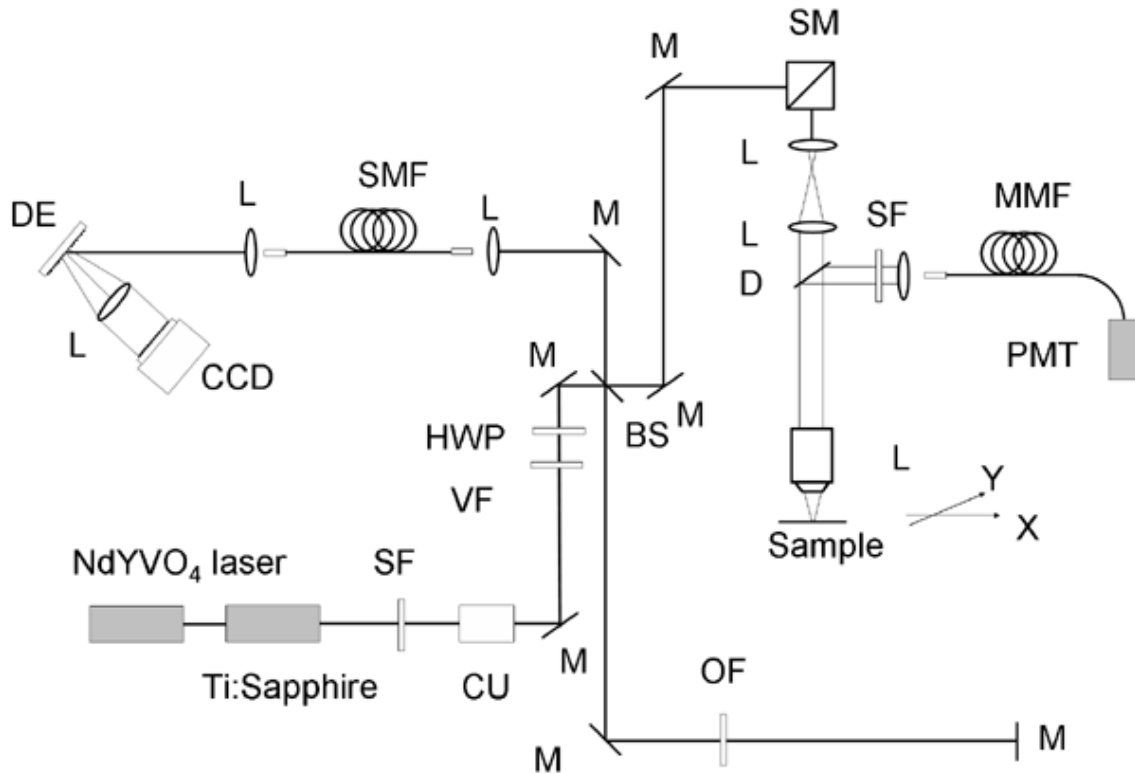


Figure 1: Experimental Setup for the integrated OCM-MPM microscope. M, mirror; SM, scanning mirrors; SF, spectral filter; L, lens; BS, beam splitter; OF, optical filter; HWP, half wave plate, SF, spatial filter; VF, variable filter; D, dichroic beamsplitter; SMF, single-mode fiber; MMF, multimode fiber; DE, diffraction grating; CU, collimating unit; PMT, photomultiplier tube.

The emitted photons that results from the two photon absorption process are emitted over the entire  $4\pi$  solid angle. A portion of the signal is collected in the backward direction by the objective and deflected by a dichroic beam-splitting mirror. The photons are then collected by a collecting unit that consist of a lens with a special housing and coupled into a multi-mode fiber. This configuration is particular useful because it allows to deliver the photons to different detection units if the case, without modifying the original setup. A filter is present too in the collecting unit in order to filter out some scattered pump. The filter can be easily replaced, which is particularly useful when we want to do two photon microscopy on different selected chromophores. For the detection of the emitted photons that results from the two photon absorption process, we use a photon counting photomultiplier tube (Hamamatsu, H7421-40) working in photon counting mode.

The photomultiplier tube detection unit is a self-contained assembly with a metal housed photomultiplier tube having a GaAsP/GaAs photocathode and a thermoelectric cooler to reduce the thermal noise. The maximum quantum efficiency corresponds to 40% at peak wavelength and the dark counts to a typical value of 100. To note that in contrast to a normal photomultiplier tube this unit does not produce an analog voltage proportional to the light intensity, but instead the output signal corresponds to a TTL signal, with each pulse corresponding to each photon detected. A picture of the imaging part of the system (galvanometer-controlled mirrors, telecentric system, imaging objective, and moving stage) is shown in Fig. 2(1).

The OCM detection scheme is different with respect to the one previously proposed by Beaufort, *et al.*<sup>4</sup>. We have implemented a spectral-domain OCM system, instead of time-domain OCM, with many different advantages. While standard OCM requires two scans to be performed (axial and lateral scanning), the spectral-domain technique can be implemented using only lateral scanning. Moreover, SD-OCM inherently provides direct access to the spectral information for spectroscopic OCM signal analysis. In addition, it has been recently shown<sup>5</sup> that the spectral-domain configuration provides significant advantages in terms of acquisition speed, sensitivity, and simplicity in the acquisition module; benefits that are incorporated into our integrated microscope. In practice, sensitivities of the order of more than 100 dB are commonly achieved with acquisition speed in the range of 30,000 spectral acquisitions per second.

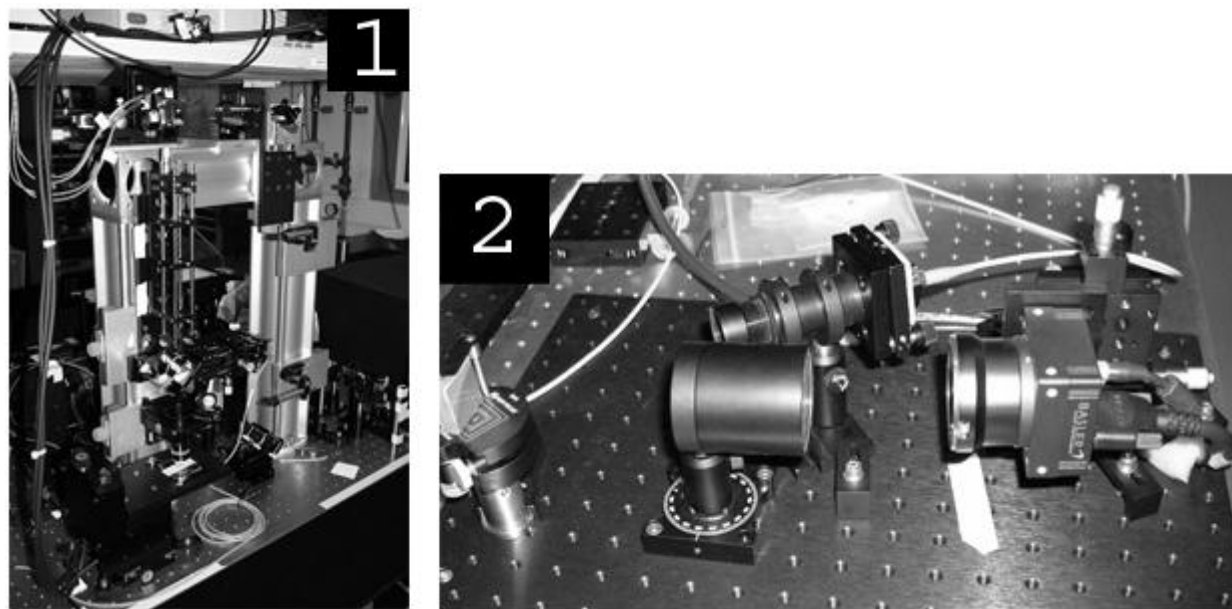


Figure 2: (1) Telecentric imaging system and imaging objective. (2) Spectral interferometric detection.

We also emphasize that the absence of any moving reference arm in the setup provides an inherent phase stability and makes this modality ideally-suited for the evaluation of the spectral components in the interference pattern. In fact, because different tissue structures and molecules have different spectral absorption and scattering properties, the spectral analysis increases the OCM image contrast, with the potential for generating spatial maps of molecules within the sample.

In our setup, light is collimated and dispersed off of a blazed diffraction grating having 830.3 grooves per millimeter. The optical spectrum is focused using a pair of achromatic lenses which have a combined focal length of 150 mm. The focused light is incident on a line-scan camera (L104k-2k, Basler) which contains a 2048-element CCD array of detection elements. This camera has a maximum readout rate of 29 kHz, thus one axial scan can be captured during an exposure interval of 34  $\mu$ s. Digital processing of the detected signal included a Spline interpolation to make the signal more uniform and a discrete Fourier transform on each set of 2048, 10-bit, values captured by the CCD to transform the signal from the frequency (spectral) domain into the spatial (depth) domain. The scattering amplitudes corresponding to the focus in each adjacent axial scan were subsequently assembled into 2D *en face* images for visualization on a personal computer. Acquisition and visualization of OCM and MPM images was performed simultaneously. A photograph of the experimental spectral interferometric detection setup is shown in Fig. 2(2).

For the electronics of the system, 2 synchronized personal computers (PCs) were used for controlling the system. One PC acquired and processed the MPM images, while the other acquired and processed the OCM images. Different controllers and electronics devices were designed in order to monitor the image scanning process in real-time. A picture of part of the electronics and controllers is shown in Fig. 3.

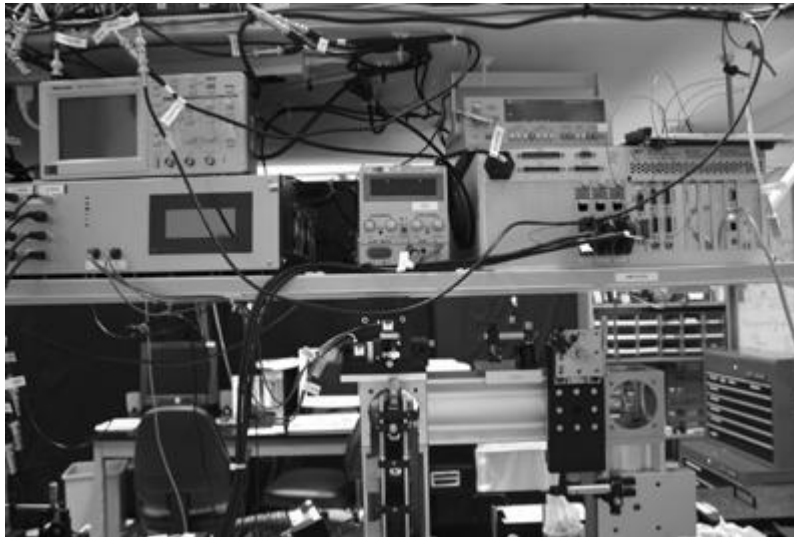


Figure 3: Electronics for controlling the combined OCM-MPM imaging system.

### 3. EXPERIMENTAL RESULTS

Figure 4 shows the axial point-spread functions of the OCM with our focusing objective, compared with the one measured when the system is operating in confocal mode using a standard PMT for the detection, instead of the CCD. Because the source spectrum is roughly Gaussian the sensitivity of OCM to the retroreflected light decreases exponentially with axial distance. The resolution is found to be equal to 2  $\mu$ m at FWHM. Note that in our system, the confocal gating is always below (higher resolution) the coherence gating, having a laser source with a bandwidth of 40 nm.

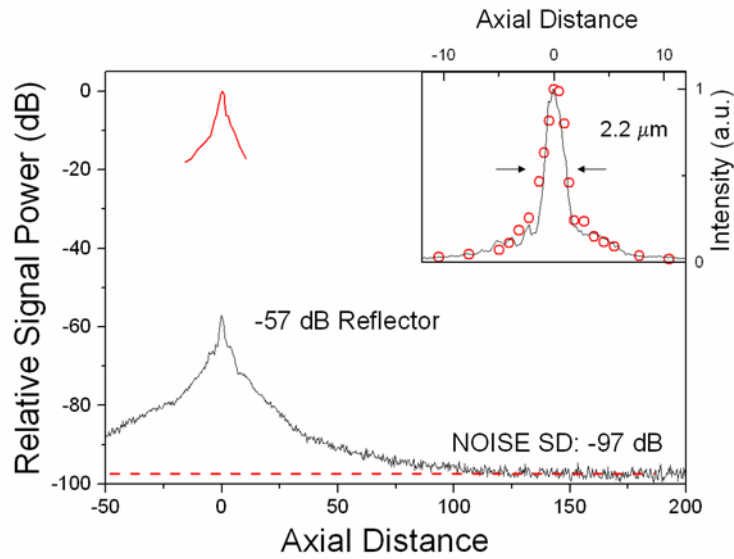


Figure 4: Sensitivity measurements of the system in OCM mode (black) and in confocal mode (red). Inset: Axial resolution measurements of the system.

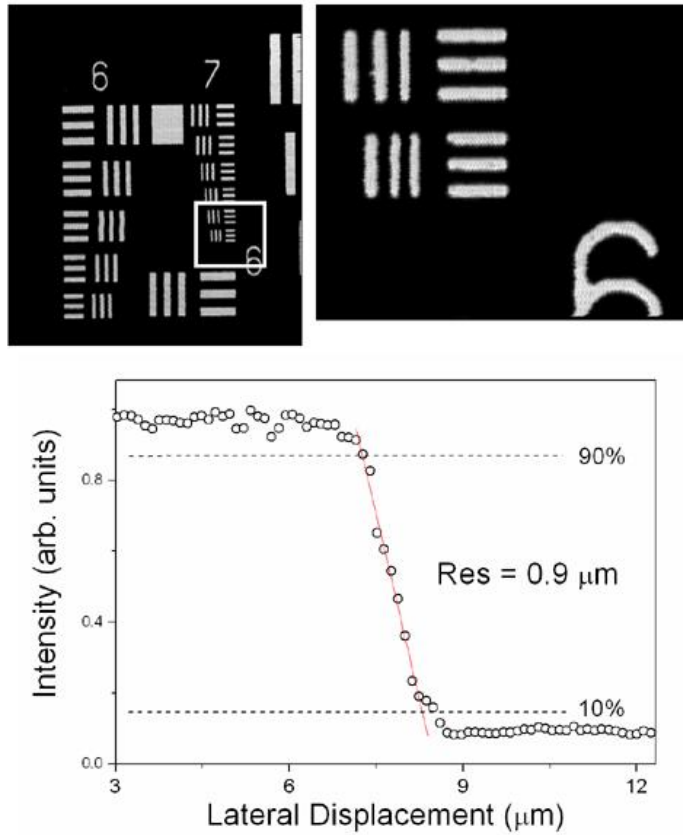


Figure 5: Lateral resolution measurements of the OCM system (USAF target). Left image size (300x350 μm). Right image size (60x50 μm).

For the sensitivity of our system, we recorded the OCM point-spread function from a mirror that was scanned through the focal plane, with a calibrated attenuation inserted in the sample arm. The SNR was calculated by taking the ratio between the signal power and the noise variance. With a 1-mW (0 dBm) power on the mirror, the measured SNR was found to be equal to 97 dB.

In Figure 5, we show an OCM image that demonstrates the high transverse resolution. The smallest elements on the standard U.S. Air Force test target is equal to  $11 \times 2.2 \mu\text{m}$ . By use of the edge scan definition, we measured a transverse resolution of less than  $0.9 \mu\text{m}$ .

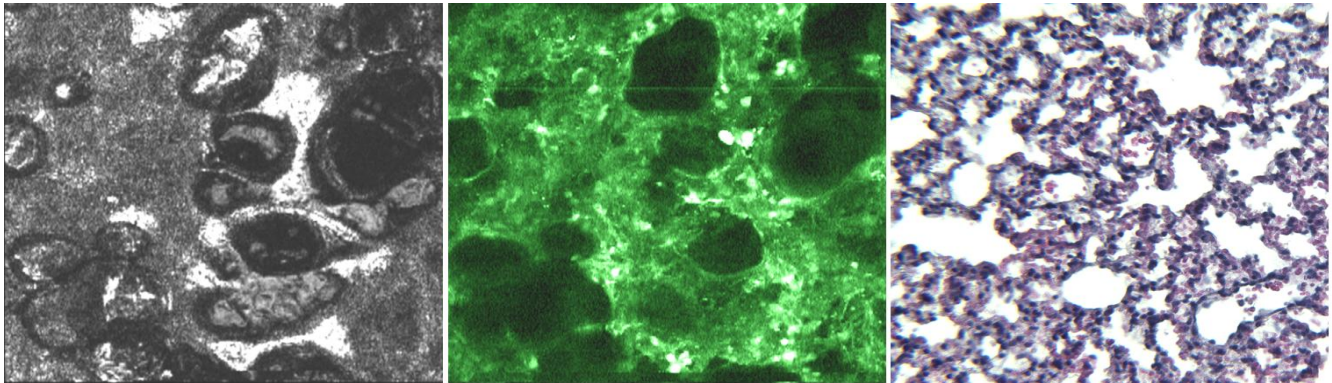


Figure 6: From left to right: OCM, MPM, and histology of lung tissue from a transgenic mouse expressing GFP (300x300 microns).

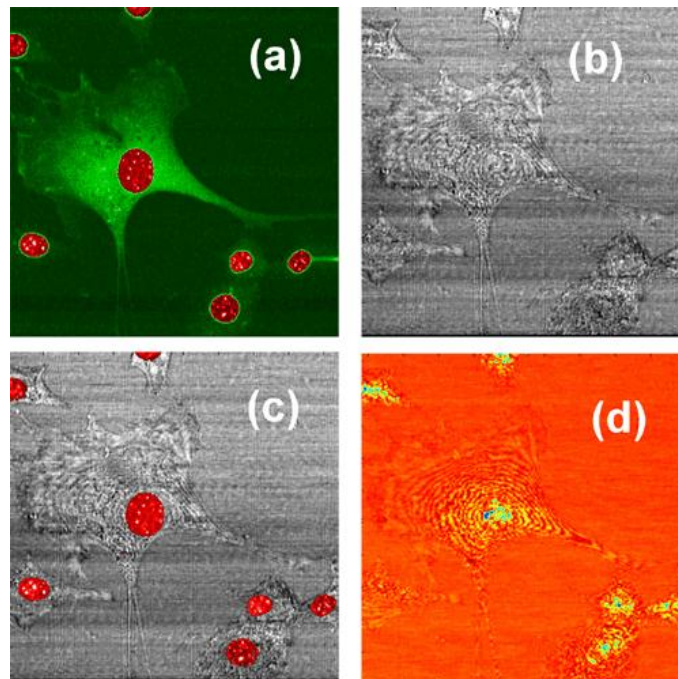


Figure 7: Single-cell images. (a) MPM, (b) OCM, (c) OCM with overlaid MPM signal from nuclei, and (d) Spectroscopic OCM of fibroblasts expressing GFP and co-stained with a dye targeted to the nucleus. Note the use of spectroscopic OCM for indicating locations identified as nuclei in MPM. Images are  $60 \times 50$  microns in size.

As mentioned in the introduction, our system integrates multiple modalities. Here we show representative images from several ongoing studies. In particular, we have implemented our system for the study and imaging of transgenic mice expressing GFP. In Fig. 6, images from the lung of a GFP mouse are presented. The OCM and MPM data are both in accordance with the histological data (OCM and MPM were taken from the same area simultaneously; histology was taken on a morphologically-similar area). In Fig. 7, we show single-cell images of cultured fibroblasts. The cells are expressing GFP-vinculin (a cell adhesion protein) and the nuclei are stained with a second dye for specific localization of nuclei relative to the cell and surrounding structures. The spectroscopic analysis of the OCM data is consistent with the MPM information, identifying the locations of the nuclei.

Functional information of cell dynamics and cell-cell and cell-scaffold interactions can be obtained, such as tracking nuclei and the expression of focal adhesion molecules such as vinculin. To demonstrate these capabilities, fibroblast cells transfected with GFP-labeled vinculin and stained with a nuclear dye (Hoechst 33342) were seeded and cultured on a microtextured poly(dimethyl siloxane) (PDMS) substrate. The microtextured PDMS consisted of 25 $\mu$ m high and 25 $\mu$ m wide microgrooves, separated by 100 $\mu$ m wide ridges<sup>6</sup>. Mechanical stimuli provided through surface textures (surface topographies) have been reported to influence cell shape, gene expression, protein production and deposition, cell proliferation, migration, differentiation, and survival. Therefore, exploring the effects of microscale textures at the cell-scaffold interface provides an attractive approach to enhance cell behavior without destabilizing the delicate biochemical condition<sup>6</sup>. OCM data demonstrates the structural information of the cell and scaffold, while the MPM images reveal the localization of the nucleus and the expression of the GFP-labeled vinculin<sup>6</sup>. The combined OCM-MPM images provide complementary and additive information regarding the cell in relation to its local environment.

A subsequent advantage of our instrument is that it allows for 3D visualization of engineered or native tissues by volume rendering a series of cross-sectional MPM and OCM images, permitting both morphological and functional assessments at the cellular and molecular levels in 3D, overtime, and under a wide variety of experimental conditions. As an example, another application involves the use of the integrated microscope to dynamically study cell-scaffold interactions under more physiological three-dimensional conditions, as shown in Fig. 8. Here, fibroblast cells were cultured in a three-dimensional Matrigel matrix. The OCM image shows the 3D cell morphology and position as well as the fibrous network of the matrix. The MPM image shows the cell nuclei and the GFP-vinculin expression in the cells. Compared to the elongated oval-shaped fibroblast cells cultured in two-dimensional cell culture, cells in 3D Matrigel display a rounded-morphology and circular nuclei. Because the Matrigel is composed of laminin and collagen IV and lacks many of the proteins associated with cell adhesion, vinculin is not as highly expressed, and the 2-photon fluorescence resulting from interactions between the cells and Matrigel is minimal<sup>6</sup>.

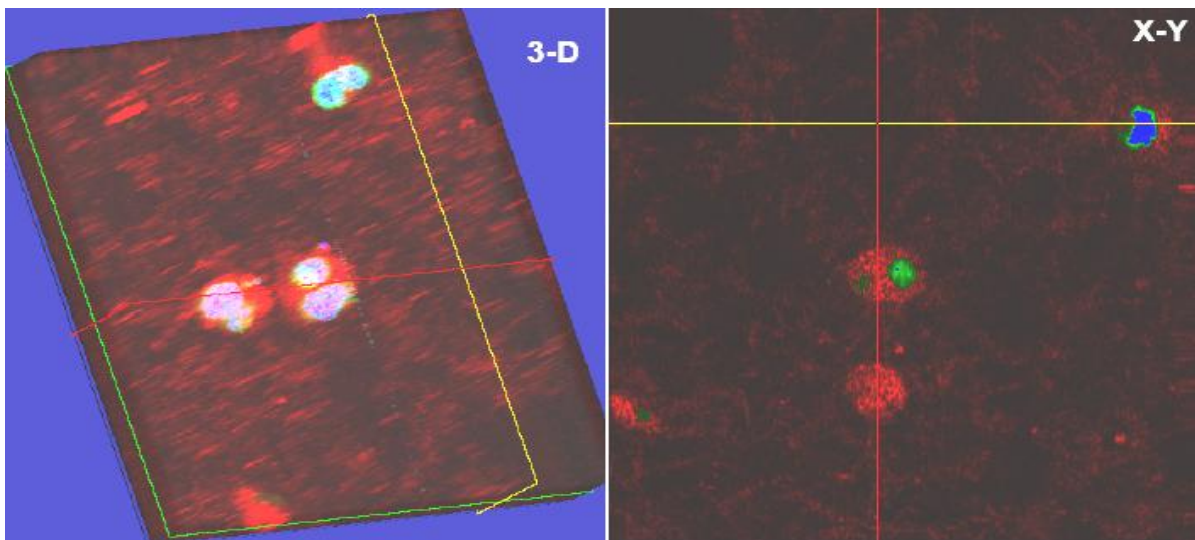


Figure 8: Fibroblast cells cultured in a 3D Matrigel matrix. Green: MPM signal from GFP-vinculin; Blue: MPM signal from nuclear dye; Red: OCM backscattered signal from matrix. Image sizes are 200 x 200 microns.

## 4. CONCLUSIONS

In conclusion, we have developed and applied an integrated microscope that is capable of simultaneous image acquisition from multiple optical imaging modalities. In this paper, we have highlighted the use of spectral-domain OCM and MPM for the detection of structure and function, respectively. The use of spectral-domain OCM allows for the visualization of background morphology and spectroscopic analysis of tissue composition, while the use of MPM permits the visualization of biological function (in this case, GFP-labelled vinculin). This instrument provides a new investigational tool for the visualization of structure and function in fields such as tissue engineering and tumor biology.

## REFERENCES

- [1] J. Bredfeldt, C. Vinegoni, D. L. Marks, S. A. Boppart, "Molecularly sensitive optical coherence tomography," *Opt. Lett.*, **30**, 495, (2005).
- [2] W. Denk, J. Strickler, W. Webb, "Two photon laser scanning fluorescence microscopy," *Science*, **248**, 73, (1990).
- [3] J. Izatt, M. Hee, G. Owen, E. Swanson, J. Fujimoto, "Optical coherence microscopy in scattering media," *Opt. Lett.*, **19**, 590, (1994).
- [4] E. Beaurepaire, L. Moreaux, F. Amblard, and J. Mertz, "Combined scanning optical coherence and two-photon-excited fluorescence microscopy," *Opt. Lett.*, **24**, 969, (1999).
- [5] R. Leitgeb, C. Hitzenberger, and A. Fercher, "Performance of Fourier domain vs. time domain optical coherence tomography," *Opt. Exp.*, **8**, 889, (2003).
- [6] C. Vinegoni, T. Ralston, W. Tan, W. Luo, D.L. Marks, S.A. Boppart, "Integrated structural and functional imaging combining spectral-domain optical coherence and multiphoton microscopy," Submitted. Downloadable from LANL E-print arXive <http://www.arxiv.org/abs/physics/0512161> (2005).